RAPID COMMUNICATIONS

PHYSICAL REVIEW B VOLUME 48, NUMBER 19 15 NOVEMBER 1993-I

Many-electron effects in BaC_{60}: Collective response and molecular effects in optical conductivity and photoionization

Göran Wendin and Bo Wästberg
Institute of Theoretical Physics, Chalmers University of Technology, S-412 96 Göteborg, Sweden
(Received 24 August 1993)

The optical conductivity of BaC_{60} is calculated using a model of an atom embedded inside a finite shell of jellium. The investigations are carried out within the framework of time-dependent local-density theory. The optical conductivity of C_{60} shows a strong collective resonance (plasmon) at 17.6 eV, which is nearly degenerate with the Ba $5p$-d giant dipole resonance, leading to strong interference effects in BaC_{60}. Molecular multiple-scattering effects appear as prominent oscillations in the Ba $4d$ photoionization spectrum of BaC_{60}, without any reduction of the overall intensity of the collective $4d$-f giant dipole resonance. The oscillations also show up in the various partial photoionization cross sections of the central Ba atom *and* the C_{60} shell.

Fullerenes represent a class of carbon molecules forming structures consisting of curved sheets of carbon, the first known molecular form of pure carbon being isolated. The closed form of these molecules is built up by carbon atoms forming 12 pentagonal rings and a varying number of hexagonal rings. The C_{60} molecule with a structure of a truncated icosahedron is a good example of this novel form of carbon. These spherical balls exhibit a remarkably high stability and may be very useful in materials science, particularly when they are mixed with small quantities of other atoms. The dopant atoms can be located either outside the cage producing fullerite salts, or inside the cage, or as a part of the cage itself replacing one or more carbon atoms. Examples of all three types of doping have already been observed experimentally.[1]

In this paper we shall focus on collective effects in optical absorption of the metallofullerene $Ba@C_{60}$ where the Ba atom is confined inside the hollow carbon cage, and on the interplay between excitations on Ba and the surrounding carbon atoms. Dynamical screening plays an important role in atomic inner-valence-shell collective excitations known as giant dipole resonances,[2-5] and the valence $5p$-d and the inner-valence $4d$-f resonances in Ba are good examples. Embedding an atom in a complex molecular or solid structure will lead to changes in optical absorption, e.g., in the form of shape resonances,[5] and it is important to understand the physical origin of these differences.

The Ba $4d$-f resonance is an atomic inner-shell resonance which may be perturbed by the molecular potential, primarily via the energy dependence of the photoelectron transmission probability. However, it has lately been claimed that atomic $4d$-f giant dipole resonances can completely collapse in a cluster environment, as suggested by an experimental study of antimony clusters by Bréchignac *et al.*[6] and a time-dependent local-density-approximation (TDLDA) calculation by Puska and Nieminen.[7] The result of our study contradicts such a notion: the Ba $4d$-f resonance *does not collapse* in our model of BaC_{60}, and the cluster environment only results in pronounced oscillations of the absorption cross section. In fact, we cannot imagine any situation where chemical effects could make this atomically localized excitation disappear.

The model used in this work is the TDLDA applied to an atom embedded inside a spherical jellium shell with the C_{60} carbon nuclei and the $1s^2$ electrons smeared out to an effective spherical surface charge. The TDLDA method has previously been applied to jellium-shell models of C_{60} (Ref. 8) and BaC_{60}.[7] The studied phenomena have been collective plasmon excitations at low energies[7,8] and dynamical screening in inner-shell photoabsorption.[7] Both aspects will be discussed in this work. Our results for isolated C_{60} represent a check on previous results, and our results for the interplay of collective electron dynamics and multiple scattering in BaC_{60} are new.

Effects of dynamical screening can be introduced by self-consistent linear-response theory in combination with the local-density approximation (see, e.g., Refs. 3 and 4). The C $2s^2$ and $2p^2$ electrons are treated as delocalized valence electrons in an effective background potential of the nuclei and the $1s^2$ core forming a homogeneously charged shell (surface charge). For BaC_{60} a central nuclear charge $Z=56$ is added. The self-consistent electronic structure is obtained by solving the density-functional (DF) Kohn-Sham equation[9] for the valence electrons using the Gunnarsson-Lundqvist local exchange-correlation potential.[10] We have chosen $N=232$ for C_{60} (instead of using all available 240 valence electrons), which gives a closed shell structure. The self-consistent solution, using the jellium-shell model for C_{60}, produces a spherical potential well and a corresponding electron distribution on the shell.

When discussing electronic properties and bonding of C_{60} it is useful to relate the electronic states to σ and π states of a planar graphite surface. Orbitals that have no radial nodes can be classified as σ states ($n=1$) and the orbitals having one node at the spherical surface as π states ($n=2$), where the $n=2$ orbitals are more extended in the radial direction. The level ordering of the $N=232$

jellium-shell model is

$$1s^2 1p^6 1d^{10} 1f^{14} 1g^{18} 1h^{22} 1i^{26} 1j^{30} 1k^{34} 2s^2 2p^6 1l^{38} 2d^{10} 2f^{14} .$$

The energy-level spectrum of the C_{60} jellium-shell model is presented in Fig. 1. The orbitals with $n=1$ are occupied up to $l=9$ and orbitals with $n=2$ are occupied up to $l=3$. The highest occupied molecular orbital–lowest unoccupied molecular orbital (HOMO-LUMO) gap of 1.8 eV for C_{60} is somewhat lower than molecular [linear combination of atomic orbitals (LCAO)] local-density results,[11] and the jellium shell model also gives a wider energy spread of occupied levels.[11]

The number of discrete low-energy valence excitations is very limited, due to the spherical symmetry, and only the $2f$-$2g$ (2.14 eV), $2p$-$3s$ (5.33 eV), $1l$-$1m$ (5.88 eV), $2s$-$3p$ (7.31 eV), and $2p$-$3d$ (7.48 eV) transitions are allowed for ≤ 10 (eV). The next possible transitions are $1i$-$2h$ (22.25 eV) and $1h$-$2g$ (23.80 eV), leaving the $\hbar\omega = 10$–20 eV region without any discrete transitions. The orbitals with π character are distributed in the energy region above -10 eV, which is similar to molecular local-density results.[11] The levels are slightly shifted when going from C_{60} to BaC_{60} and the Ba $6s^2$ electrons are transferred to C_{60}.

The static polarizability of our C_{60} jellium-shell model is $\alpha(0)=138$ Å^3. This value is considerably higher than the tight-binding result 37 Å^3 of Bertsch *et al.*[8] and the quantum chemical result of 44–65 Å^3,[12] but is similar to the random-phase approximation (RPA) jellium model result of Bertsch *et al.*[8] These results should be compared with the classical result $\alpha(0)=R^3=46$ Å^3 for a conducting sphere and the recent experimental results for C_{60}, $\alpha(0)=79.3$–85.2 Å^3.[13,14] The TDLDA calculation of Puska and Nieminen,[7] with a square-well-like *model* potential, quite different from ours, gave $\alpha(0)=92$ Å^3, considerably lower than our result but close to experiment.

Figure 2 (dashed line) shows the TDLDA photoabsorption cross section (proportional to optical conductivity) for the C_{60} jellium-shell model for photon energies above the first ionization threshold at 4.5 eV. The spectrum is

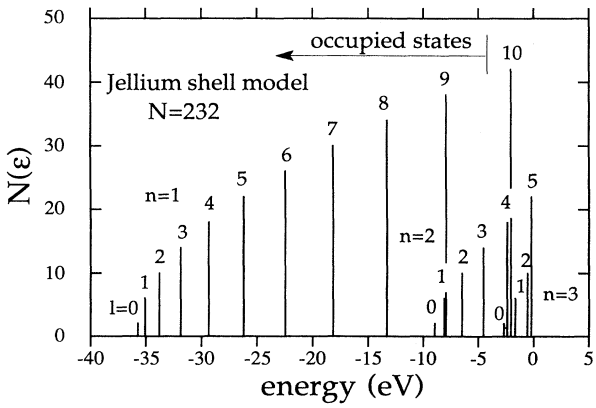

FIG. 1. One-electron energy spectrum of the jellium-shell model with $N=232$ electrons and the radius $r=6.78a_0$. The heights of the bars represent the $2(2l+1)$ degeneracy of the electronic states.

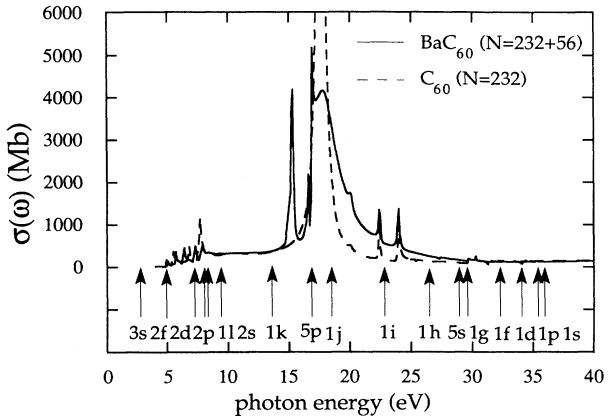

FIG. 2. The calculated photoabsorption cross sections for a jellium shell with $N=232$ (C_{60}) (dashed line) and for a Ba atom ($Z=56$) embedded in a jellium shell with $N=232$ (BaC_{60}) (solid line) using the TDLDA method. At the bottom of the figure, the thresholds for photoemission from the various occupied shells of Ba and C_{60} have been marked with arrows.

dominated by a giant dipole resonance, a dipolar collective plasmon ($\sigma+\pi$) resonance with a maximum at $\hbar\omega=17.6$ eV (σ oscillating in phase with π), and with the largest contribution from the π shell. The 5–8-eV resonances may be characterized as dressed single-particle $2p$-$3s$, $1l$-$1m$, $2s$-$3p$, and $2p$-$3d$ transitions interacting with the collective ($\sigma-\pi$) system. Additional resonances occur at 22.5 and 23.3 eV and are probably best characterized as dressed and shifted $1i$-$2h$ and $1h$-$2g$ single-particle excitations interacting with the neighboring ($\sigma+\pi$) plasmon resonance.

Since this paper is focused on BaC_{60}, we shall only very briefly mention some of the theoretical[8,7,15,16] and experimental[17,18] results for C_{60}. We first note that our result for the jellium shell in the 0–40-eV region looks very similar to the jellium-shell RPA results of Bertsch *et al.*,[8] but quite different from the TDLDA jellium-shell result of Puska and Nieminen[7] (whose potential is square-well-like). On the experimental side, Sohmen, Fink, and Krätschmer[17] have derived the optical conductivity $\sigma(\omega)$ from electron-energy-loss spectroscopy (EELS) for a thin film, finding a very intense and broad, structured, "flat-top" peak which is centered around 17–18 eV. Disregarding extra-cluster local field corrections, we just note that the jellium-shell result places the giant dipole resonance at the center of the experimental conductivity peak. However, the jellium-shell peak is much more narrow than the experimental result because the local inhomogeneities due to the atomic and molecular structure of C_{60} are absent. The photoion yield (PIE) result of Hertel *et al.*[18] for a beam of neutral C_{60} has the same peak structure as $\sigma(\omega)$ from EELS,[17] but the overall shape and the center of gravity are not at all the same. Unless branching into fragmentation channels is very important, the PIE should be proportional to $\sigma(\omega)$. We conclude that the photoabsorption cross section for the giant dipole resonance measured on a *free* C_{60} molecule still involves considerable uncertainties.

The BaC_{60} cross section in the 0–40-eV region, shown in Fig. 2 (solid line), involves a complicated mixture of the nearly degenerate collective Ba $5p$-d and C_{60} giant dipole resonances, leading to various modes of combined oscillations and to prominent interference effects. The structure becomes quite dramatic in this clean case of Ba in the jellium shell. However, similar effects should be observable also in the real BaC_{60} system. We suggest that the peak at 15.3 eV represents a collective mode where the Ba $5p$ shell and the C_{60} shell move in opposite ways, 180° out of phase. This collective resonance may be mixed with the single-particle $5p$-$3d$ excitation (14.86 eV). The more intense structure around 17–19 eV should represent in-phase motion of the Ba $5p$ shell and the C_{60} shells (cf. Ref. 4). Moreover, since the resonance sits above the Ba $5p$ ionization threshold, it will be broadened in comparison with C_{60} and will also include Ba $5p$ emission. In addition, there are some single-particle-like transitions driven by and modified by the collective field, with clear differences between C_{60} and BaC_{60}.

The photoabsorption cross section (optical conductivity) of BaC_{60} (Ba in the jellium shell) in the 90–160-eV region, above the Ba $4d$ threshold, is shown in Fig. 3(a). The C_{60} shell can disturb the central Ba in basically two ways: (i) through hybridization of Ba and C_{60} wave functions and (ii) through multiple scattering by the shell potential, altering the energy-dependent transmission properties of photoelectrons.

The effect of the Ba-C_{60} hybridization can be seen in the relatively strong BaC_{60} $4d$-$6p$ resonance at 90 eV and $4d$-$4f$ resonance at 92 eV, resonances which practically vanish in the Ba atom.[19] Otherwise, the influence of the C_{60} shell on the $4d$ polarization is very small despite the Ba-C_{60} hybridization changing the wave functions of the occupied and empty states in the valence region. Such effects will show up more clearly in the partial, level-specific, photoionization cross sections.

Concerning the Ba $4d$-f giant dipole resonance, the concept of hybridization becomes ill-defined and it is better to talk about multiple scattering and energy-dependent transmission through the C_{60} shell region. A very clear message from Fig. 3(a) is that the effect of the C_{60} shell is to induce an oscillation in the cross section without changing the overall atomic shape and strength. The effect of the induced potential may be represented as an effective $l=3$ repulsive one-electron potential which contributes to a potential barrier inside the usual Ba f-electron angular momentum barrier.[20] This core region cannot be influenced by any type of *chemical* environment. Since the giant dipole resonance f-continuum wave function resonates in this inner-well region (that is why it is often labeled "$4f$"), the effective $4d$-"$4f$" dipole moment cannot be changed by chemical means. However, since the "$4f$" wave function is not confined by a barrier—it is just partially reflected at the border between the core region and the outer "valence" region, like resonances in an open organ pipe—it will be more or less heavily influenced by the energy-dependent transmission and reflection properties of the chemical surrounding. This multiple-scattering effect is the main source of the oscillations seen in the BaC_{60} cross section (which cannot be described in terms of extended x-ray-absorption fine structure and single scattering).[21]

Finally, corresponding results for the effects of resonant photoemission on partial photoionization cross sections are shown in Figs. 3(a) and 3(b). The giant dipole resonance is primarily associated with the $4d$-f partial cross section [Fig. 3(a)]; resonant contributions in other channels [Fig. 3(b)] may be seen as due to the electric field of the oscillating induced $4d$-f charge or may be regarded as effects of autoionization of the resonance into other channels. A new feature is that the oscillations of the giant dipole resonance also appear in, e.g., the $5p$ and $5s$ partial cross sections in Fig. 3(b). Another new feature is that we can see the pronounced effects of resonant photoemission from the "ligand" C_{60} shell. A more detailed discussion of partial cross sections and resonant photoemission will be given in future work.

In conclusion, within the TDLDA we have calculated the dynamic response of Ba in the jellium shell, approxi-

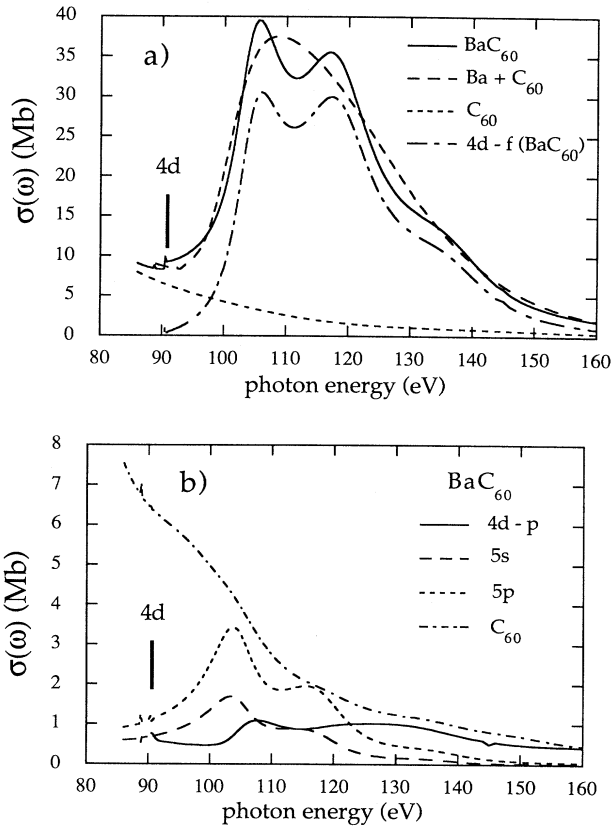

FIG. 3. Photoabsorption cross sections of Ba and BaC_{60} showing the $4d$-f giant dipole resonance. The cross sections were calculated using the TDLDA method for a Ba atom and for Ba in a jellium shell ($N=288$). (a) shows the BaC_{60} cross section compared to the cross section of the Ba atom plus the $N=232$ jellium-shell model for C_{60} and the $4d$-f partial cross section of BaC_{60}. (b) shows the $4d$-p, the $5s$-p, and the $5p$-$s+5p$-d partial cross sections and the contribution from C_{60} states to the total cross section of BaC_{60}.

mating C_{60} by a jellium shell and describing collective excitations as well as effects of multiple scattering. A characteristic for the jellium shell is the very sharp and well-defined giant dipole resonance (plasmon) around 17 eV (without any trace of splitting due to modes associated with the inside and outside of the shell). In contrast, photoionization experiments on real C_{60} suggest that the plasmon is fairly broad and structured. This increased damping and structure is a consequence of the short-range inhomogeneities in the real C_{60} molecule.

Introducing a central Ba atom inside our model C_{60} shell leads to complicated collective behavior in the 5–30-eV region involving mixtures of the Ba $5p$-d giant dipole resonance and the C_{60} dipolar plasmon mode. These modes are practically degenerate, and the structure becomes quite dramatic in this clean case of Ba in the jellium shell. However, similar effects should be observable also in the real BaC_{60} system.

In the 100-eV region the response is dominated by the 25-eV broad Ba $4d$-f giant dipole resonance. The C_{60} shell does not in any way change the overall intensity of this resonance. However, the radial shell does modulate the transmission probability of the photoelectron, leading to pronounced oscillations of the photoabsorption cross section depending on the precise form of the C_{60} potential. Finally we just note that the cross sections in Figs. 3(a) and 3(b) are very similar to experimental photoyield and resonant photoemission data for YBaCuO.[22–24]

Note added in proof. The authors of Ref. 7 have kindly informed us that they now agree with the results of the present paper.

[1]R. E. Smalley, in *Large Carbon Clusters,* edited by G. Hammond and V. Kuck, ACS Symposium Series, 1991 (American Chemical Society, Washington, D.C., 1992).
[2]G. Wendin, Phys. Lett. **51A**, 724 (1975).
[3]A. Zangwill and P. Soven, Phys. Rev. A **21**, 1561 (1980).
[4]G. Wendin, Phys. Rev. Lett. **53**, 724 (1984).
[5]*Giant Resonances in Atoms, Molecules, and Solids,* edited by J. P. Connerade, J. M. Esteva, and R. C. Karnatak (Plenum, New York, 1987).
[6]C. Bréchignac *et al.*, Phys. Rev. Lett. **67**, 1222 (1991).
[7]M. J. Puska and R. M. Nieminen, Phys. Rev. A **47**, 1181 (1993).
[8]G. F. Bertsch, A. Bulgac, D. Tomanek, and Y. Wang, Phys. Rev. Lett. **67**, 2690 (1991).
[9]W. Kohn and L. J. Sham, Phys. Rev. **140**, A1133 (1965).
[10]O. Gunnarsson and B. I. Lundqvist, Phys. Rev. B **13**, 4274 (1976).
[11]B. Wästberg, Phys. Scr. **44**, 276 (1991).
[12]P. W. Fowler, P. Lazzaretti, and R. Zanasi, Chem. Phys. Lett. **165**, 79 (1990).
[13]S. L. Ren *et al.*, Appl. Phys. Lett. **59**, 2678 (1991).
[14]H. Cohen, E. Kolodney, T. Maniv, and M. Folman, Solid State Commun. **81**, 183 (1992).
[15]D. Östling, P. Apell, and A. Rosén, Europhys. Lett. **21**, 539 (1993).
[16]E. Westin and A. Rosén (unpublished).
[17]E. Sohmen, J. Fink, and W. Krätschmer, Z. Phys. B **86**, 87 (1992).
[18]I. V. Hertel *et al.*, Phys. Rev. Lett. **68**, 784 (1992).
[19]The present calculation is nonrelativistic and non-spin-polarized. Therefore, the true $4d$-$4f$ transition around 92 eV is very weak. If we include energy splitting of the $4d$ shell into $4d_{5/2}$ and $4d_{3/2}$ subshells within the TDLDA a small but prominent $4d$-$4f$ "^3D" will appear (Ref. 4) in agreement with experiment.
[20]Z. Crljen and G. Wendin, Phys. Rev. A **35**, 1555 (1987); **35**, 1571 (1987).
[21]We have repeated the calculation using the potential of Puska and Nieminen (Ref. 7), which is more like a square well. We find no essential difference in comparison with Fig. 3(a): There is only a little more structure due to the sharper wells of the potential, much like the earlier result of Wendin, quoted by Puska and Nieminen (Ref. 7). We have to conclude that something went wrong in Ref. 7. (The same problem also concerns the result for XeC_{60} in Ref. 7.)
[22]M. Onellion *et al.*, Phys. Rev. B **36**, 819 (1987).
[23]Z.-X. Shen *et al.*, Phys. Rev. B **36**, 8414 (1987).
[24]K.-L. Tsang *et al.*, Phys. Rev. B **37**, 2293 (1988).